TWENTYFIFTH EUROPEAN ROTORCRAFT FORUM

Paper n° G3

AEROELASTIC AND AEROSERVOELASTIC STABILITY OF THE BA 609

BY

TOM PARHAM JR., LAWRENCE M. CORSO

BELL HELICOPTER TEXTRON INC., FORT WORTH, TEXAS, USA

SEPTEMBER 14–16, 1999
ROME
ITALY

ASSOCIAZIONE INDUSTRIE PER L'AEROSPAZIO, I SISTEMI E LA DIFESA
ASSOCIAZIONE ITALIANA DI AERONAUTICA ED ASTRONAUTICA

AEROELASTIC AND AEROSERVOELASTIC STABILITY OF THE BA 609

Tom Parham, Jr.
Lawrence M. Corso
Bell Helicopter Textron, Inc.
Fort Worth, Texas, U.S.A

1. ABSTRACT

The BA 609 is a nine passenger, 16,000 lb (7,250 kg) civil tiltrotor being designed by Bell Helicopter Textron, Inc. and Agusta, a Finmeccanica Company. The BA 609 design must meet all stability requirements specified in the civil certification basis. Based on analysis and Bell's experience with previous tiltrotor aircraft, the BA 609 will meet these requirements. The first tiltrotor developed at Bell was the XV–3. During the testing of this aircraft, a coupled rotor/wing whirl instability was encountered in airplane mode. The phenomenon is similar to propeller whirl flutter, except that rotor gimbal flapping and inplane mode coupling are important factors on tiltrotor aircraft. This proprotor stability phenomenon has been an important design consideration during the XV–15 and V–22 development. At Bell Helicopter Textron, Inc., analyses and methodology for the stability analysis of tiltrotors have been developed over the last 25 years. The U.S. Marine V–22 was developed using similar stability analyses and has demonstrated speeds of 379 knots (702 km/h) in airplane mode flight. To ensure that the stability requirements are met for these aircraft, their wing stiffnesses are designed to preclude proprotor stability. On the BA 609, the wing airfoil thickness-to-chord ratio is 23% thick to achieve the stiffness requirements. Once the basic airframe is designed, the effect of the flight control system is included in the analysis. Because the V–22 and BA 609 both use high-bandwidth digital control systems, these effects must also be considered in the stability analysis. The flight control system model used for stability analysis includes pilot biomechanical models to represent the pilot control inputs caused by cockpit accelerations of the structural modes. Filters are included in the flight control system, where needed, to reduce the coupling with the structural modes. Extensive correlation of analysis with model test data and flight test data yields high confidence that the BA 609 design requirements will be met.

2. INTRODUCTION

Currently Bell and Agusta are developing the BA 609 to be the world's first civil tiltrotor. Fig. 1 shows a full-scale mockup of the BA 609. The gross weight of this aircraft is 16,000 lb (7,250 kg), significantly smaller than the V–22, which has a nominal gross weight of 47,000 lb (21,315 kg). The BA 609 is designed to provide point-to-point transportation for up to nine passengers at cruise speeds up to 275 knots (509 km/h) and at ranges up to 750 nautical miles (1,390 km). There are significant challenges in designing a tiltrotor aircraft to meet these requirements. Aeroelastic and aeroservoelastic stability must be considered early in the design process to ensure that the stability requirements are met.

Tiltrotor aircraft can experience a wing/pylon/rotor whirl instability in high-speed airplane mode similar to the propeller-whirl flutter of conventional propeller aircraft. The proprotor stability problem is more complicated than conventional propeller-whirl flutter because of the additional flapping and feathering degrees of freedom, control system flexibility, and blade kinematic and elastic couplings. The proprotor stability phenomenon was first encountered on the XV–3 tiltrotor, as described in Ref. 1. Both propeller-whirl and proprotor instabilities are a result of precession-generated aerodynamic loads, but the flapping degree of freedom of the proprotor causes fundamental differences in the instability. Bell and NASA conducted joint research on the problem, studying it with analysis and model tests (Refs. 2 and 3). This research paved the way for the successful Bell/NASA XV–15 program (Ref. 4). The XV–15 aircraft, which is similar in size and weight to the BA 609, demonstrated that tiltrotor aircraft can be designed and built with proper wing stiffness to preclude proprotor stability. The proprotor stability phenomenon continues to be studied with analysis and tests to determine other design parameters that affect stability (Refs. 5, 6, and 7).

During the XV–15 flight test program, damping in one of the antisymmetric wing modes was less than predicted when the stability augmentation system (SCAS) was on. However, with the SCAS off, damping was much higher. The problem was traced to the roll rate feedback in the SCAS, which was degrading the stability of this mode (Ref. 8). A notch filter circuit was added to the SCAS to reduce coupling with this wing mode. With

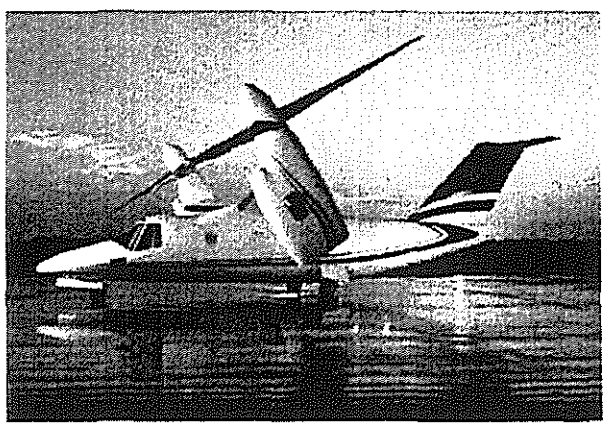

Fig. 1. BA 609 civil tiltrotor.

this filter, the damping SCAS on was similar to SCAS off. The BA 609 digital flight control system (FCS) is included in the stability analysis to ensure that the FCS does not degrade the stability of the wing modes.

In addition to the FCS, the pilot can respond at the structural mode frequencies and create an additional feedback path. Refs. 9 and 10 describe the pilot coupling phenomenon on helicopters. The pilot acts like a feedback path, causing control inputs due to cockpit accelerations of the structural modes. On large aircraft like the V–22, this can be a significant issue, because of the low-frequency structural modes. Refs. 11 and 12 describe pilot coupling on the V–22 and the design changes that reduce pilot biomechanical coupling.

3. PROPROTOR STABILITY

Airplane mode proprotor instability can be characterized as a whirl divergence as a result of precession-generated aerodynamic hub forces. The proprotor is destabilized by shear forces only, since the rotor is gimbaled to the mast. Due to the flapping degree of freedom, the proprotor destabilizing forces can create an instability in either the pitch or yaw degree of freedom alone. Ref. 13 provides a detailed discussion of this instability, which is briefly described below.

To understand the origin of the destabilizing forces, consider a proprotor and pylon undergoing a pitch oscillation. For the simplified case discussed here, the rotor consists of rigid blades with a gimbaled hub to allow rotor flapping. The swashplate, or control plane, is fixed relative to the mast. The pitch motion of the control plane will cause the rotor to process at the pylon pitch rate and assume a flapped position relative to the mast. The elemental blade forces cause an inplane shear force that causes proprotor/pylon instability at high speed. This instability is a significant design driver on tiltrotor aircraft. Specifically, the wing torsional stiffness requirements dictate that the wing be thick relative to comparable turboprop aircraft (23% for the BA 609). The high torsional stiffness associated with the thick wing design helps reduce the amount of pylon pitching motion in the fundamental wing bending mode, thereby minimizing the destabilizing effect.

4. ANALYTICAL METHODOLOGY

Fig. 2 is a flowchart showing the stability analysis methodology. Aeroelastic Stability Analysis of Proprotors (ASAP) is a linear eigenvalue analysis developed at Bell specifically for proprotor stability.

The stability analysis is first performed on the basic aircraft without including the FCS. The wing stiffnesses and pylon support and rotor properties are iterated until the requirements are satisfied. Then a linearized model for the FCS is added to the analysis to verify that the FCS does not significantly degrade the stability of the system. Structural notch filters are used to reduce FCS gain at the elastic mode frequencies as required. This methodology has been successfully used on the V–22 aircraft (Ref. 12).

The pilot can induce oscillations of the elastic modes of the aircraft through the cockpit controls. The flight control system and mechanical controls must also be designed to preclude these oscillations. In the stability analysis, the pilot/control system is modeled as a dynamic system that creates feedback paths from cockpit accelerations to control inputs. Because there is significant variability in the pilot/stick dynamic systems, the stability is evaluated with the highest gain that is expected for the pilot/control system.

5. ASAP MATH MODEL

ASAP is a linear eigenvalue stability and forced response analysis developed by Bell for tiltrotor aircraft. The analysis is based on constant coefficient differential equations. For helicopter and conversion mode, the analysis uses coefficient averaging (Ref. 14) to eliminate periodic coefficients. The analysis includes an elastic airframe, drive system, and rotor model, as well as a general FCS model.

ASAP uses discrete hinges and springs to represent the rotor system dynamics. The rotor is allowed a gimbal degree of freedom at the mast centerline, which includes

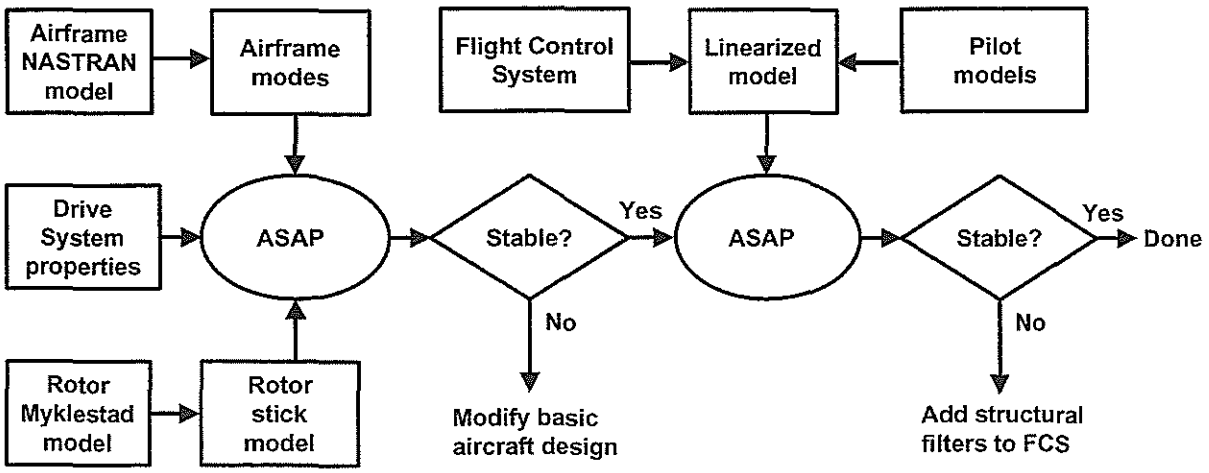

Fig. 2. Overview of tiltrotor stability methodology using ASAP.

the rotor underslinging dynamics. The analysis has provisions for discrete coning and lead-lag hinges along the blade. Fig. 3 shows the degrees of freedom for the ASAP rotor model, which allow ASAP to model the rotor cyclic flapping and inplane modes and the collective rotor coning mode. Kinematic pitch-flap, pitch-cone, and pitch-lag coupling are calculated external to the program and input in table form to represent the blade feathering motions. The blade static deformed position is represented by steady angles about the hinges, including coning at the coning hinge and prelag at the lag hinge. These steady deformations are also calculated external to ASAP and input in table form.

ASAP includes two rotor aerodynamic models. Rotor aerodynamics can be represented by a constant parameter or distributed parameter model:

1. The constant parameter model uses a constant chord blade with constant lift curve slope and assumes ideal twist. The blade lift curve slope is corrected for Mach number effects using an effective Mach number and the Prandlt Glauert correction. The rotor angle of attack at the 3/4 radius is defined in a table of angle of attack as a function of rpm and airspeed. While this rotor model is quite simplistic, it has worked well in correlation with measured stability data.
2. Alternatively, the distributed parameter aerodynamic model can be used. This model uses the actual chord distribution, twist, and airfoil tables. The blade aerodynamic coefficients are linearized about the trim position at each blade segment. Rotor trim parameters are calculated external to the analysis and input in tabular form. Typically, high-speed airplane mode stability is less sensitive to the trim condition than is helicopter mode stability.

The airframe is represented by up to twenty-five symmetric or antisymmetric airframe modes. The modal frequency, damping, and mode shape are input to the analysis. The rotor hub, control plane, control surface, and aircraft center of gravity (cg) mode shapes are provided to include coupling with the rotor forces and airframe control surface aerodynamic forces. The airframe control surfaces are represented by linear aerodynamic derivatives that act as concentrated forces on effective mode shapes for the control surfaces.

The ASAP math model includes a representation of the rotor control system geometry to model pylon/swashplate control system coupling. Blade feathering with respect to the mast is input to the rotor to account for the mast bending in the elastic mode shapes. This feathering includes the effect of rotor system phasing and geometry.

ASAP includes a drive system dynamic model with the shafts represented by torsional springs and the rotor, engine, and gearboxes represented by inertias (Fig. 4). The model includes the four torsional springs (mast, proprotor gearbox drive shaft, engine drive shaft, and interconnect drive shaft) and four inertias (rotor, engine, proprotor gearbox and tilt-axis gearbox. These degrees of freedom are adequate to represent the first symmetric and first two antisymmetric drive system modes, which can be important in calculating stability. The drive system model also includes a perturbation engine torque, so that the model can be used for torsional stability.

A general FCS model is included in ASAP for aeroservoelastic stability analysis. The FCS model has a library of linear transfer functions, which can be arranged with inputs, outputs, and summing junctions to model any linear control system. Any of the system degrees of freedom can be used as sensors to the control system. Mode shape locations are provided so that the airframe response at any point can be used as an input to the FCS. The rudder, aileron, elevator, rotor collective, rotor cyclic, and engine torque are possible control outputs. The pilot biomechanical feedback is modeled as an additional feedback in the FCS. Any nonlinear elements in the FCS are

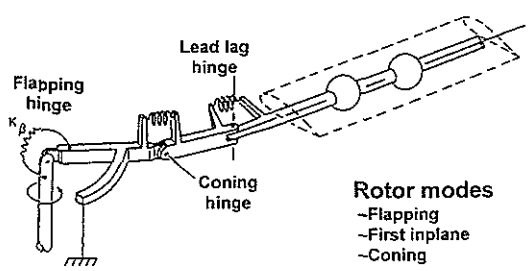

Fig. 3. ASAP rotor model.

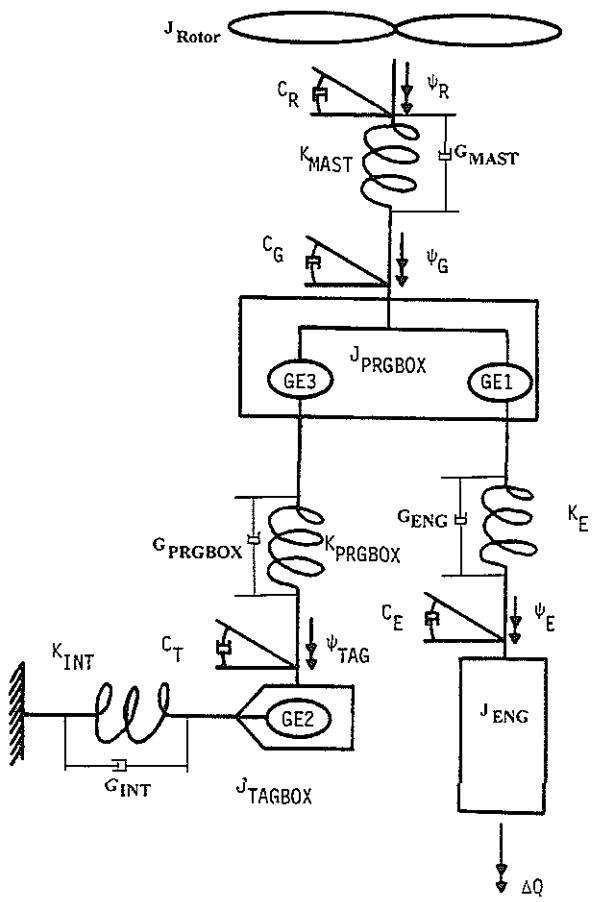

Fig. 4. ASAP drive system model.

represented by their linear equivalent. For example, digital delays are represented by second order Pade approximations.

Using the ASAP rotor, airframe, and FCS math models, several stability problems can be analyzed. The coupled rotor/airframe math model allows rotor flap/lag and wing/pylon/rotor stability to be analyzed in airplane and helicopter modes. The FCS model allows aeroservoelastic stability to be analyzed. Root locus plots as well as frequency and damping versus airspeed plots can be generated by the analysis. For control system analysis, Bode plots are generated to calculate the gain and phase margins in the FCS.

Fig. 5 shows correlation of ASAP analysis with measured stability data from Ref. 13. This data is for an early V–22 wind tunnel model and verifies that the simple ASAP rotor model is adequate for proprotor stability predictions. Ref. 12 describes the correlation of ASAP with V–22 measured stability data, including the effects of the FCS and pilot biomechanical coupling.

6. BA 609 AIRFRAME DYNAMIC PROPERTIES

Airframe dynamics are represented by a detailed NASTRAN finite-element model. The normal modes of the airframe are calculated by NASTRAN and input to ASAP. The BA 609 NASTRAN model is shown in Fig. 6. This model has approximately 38,700 grids and over 232,000 degrees of freedom. Most of the aircraft structure is modeled by plate and bar elements. CONM2 elements are used to distribute the mass and inertia properties over the structural model. Modes are generated for stability analysis at various nacelle angles and gross weight configurations.

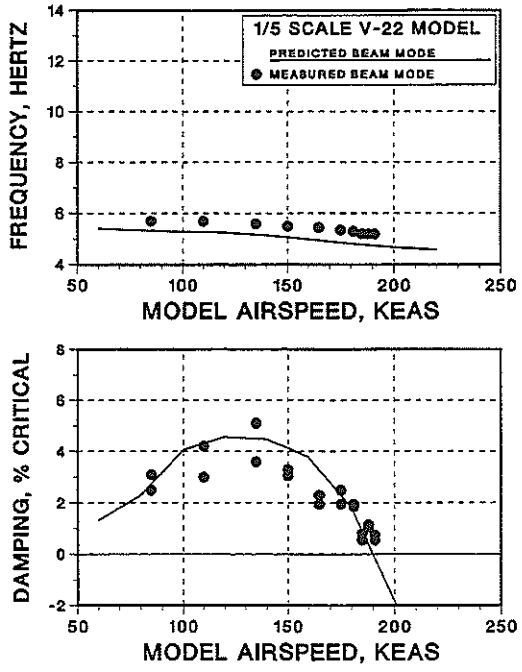

Fig. 5. Correlation of ASAP with model test data.

The airframe frequencies for airplane and helicopter modes at 16,000 lb (7,250 kg) gross weight are shown in Table 1. The six rigid body modes are calculated by NASTRAN, but are not included in the table. Each mode has a name that describes the fundamental motion. For example, the "symmetric wing beam" mode primarily involves symmetric beamwise bending of the wing. In airplane mode the pylon cg is forward of the wing elastic axis, so there is wing torsion motion in this mode also. Because of the complexity of the structure, none of the modes are purely vertical or lateral, even though they may be labeled as such. NASTRAN models the coupling between the degrees of freedom, and all mode shapes include motion in all three translation and rotation degrees of freedom.

The NASTRAN model is also used for vibration predictions and predicts the higher frequency modes up through 6/rev. For proprotor stability analysis, only the fundamental wing modes below 1/rev are important and Table 1 lists only these modes. The BA 609 FCS operates at 50 Hz, so the FCS Nyquist frequency is 25 Hz. For stability analysis including the FCS, the modes up to the Nyquist frequency are included, although the fundamental wing modes are still the critical modes.

7. BA 609 DRIVE SYSTEM DYNAMIC PROPERTIES

The drive system in the BA 609 includes engines mounted in the pylons and an interconnect drive shaft between the two rotors. The long interconnect drive shaft causes the first antisymmetric drive system frequency to be in the frequency range of the fundamental wing modes, so the drive system can be important for stability. Table 2 lists the BA 609 drive system natural frequencies.

8. BA 609 ROTOR DYNAMIC PROPERTIES

The rotor used on the BA 609 is a three-bladed, stiff-inplane rotor. The blades are tapered and highly twisted (47.5 degrees) to achieve low-speed and high-speed performance. The rotor has a constant velocity gimbal at the mast centerline to allow rotor flapping. A relatively small hub spring is used to reduce flapping

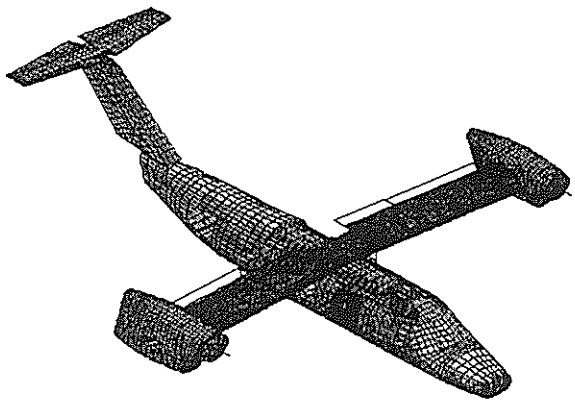

Fig. 6. BA 609 NASTRAN model in airplane mode.

Table 1. BA 609 airframe properties.

Airplane Mode (478 rpm)	Frequency		Helicopter Mode (569 rpm)	Frequency	
Mode name	Hz	*x*/rev	Mode name	Hz	*x*/rev
Symmetric wing beam	3.35	0.42	Symmetric wing beam	3.02	0.32
Antisymmetric wing chord	3.76	0.47	Antisymmetric wing chord	3.68	0.39
Symmetric wing chord	5.31	0.67	Symmetric wing torsion	4.29	0.45
Antisymmetric wing beam	5.87	0.74	Antisymmetric wing torsion	4.78	0.50
Symmetric wing torsion	6.10	0.77	Antisymmetric wing beam	6.05	0.64
Antisymmetric wing torsion	6.36	0.80	Antisymmetric pylon yaw	6.30	0.66
Fuselage lateral bending	7.35	0.92	Symmetric wing chord	6.62	0.70
Symmetric pylon yaw	10.66	1.34	Symmetric pylon yaw	6.94	0.73
Antisymmetric pylon yaw	10.88	1.37	Fuselage lateral bending	7.51	0.79
Fuselage vertical bending	12.05	1.51	Fuselage vertical bending	11.31	1.19

Table 2. Drive system natural frequencies.

Mode	Frequency (Hz)
1st antisymmetric	3.27
1st symmetric	6.70
2nd antisymmetric	9.07

Table 3. BA 609 rotor frequencies.

	Airplane Mode 478 rpm; $\theta = 87.5$ deg		Helicopter Mode 569 rpm; $\theta = 75$ deg	
Mode	Rotating system (*x*/rev)	Fixed system (Hz)	Rotating system (*x*/rev)	Fixed system (Hz)
Flapping	1.005	0	1.002	0
In-plane	1.300	2.391	1.255	2.419
Coning	1.188	9.468	1.15	10.911

during rotor startup. The constant velocity gimbal is used to reduce the drive system 2/rev torque when the rotor flaps. The design uses negative δ_3 (flap up, pitch nose up) to reduce flapping and keep the rotor flapping mode below 1/rev to eliminate the possibility of flap/lag instability (*Ref. 15*). For proprotor stability, only the fundamental rotor modes are significant, and only these modes are modeled in ASAP. Table 3 shows the fundamental rotor frequencies (no aerodynamics or airframe coupling) at two different rotor speeds. The BA 609 operates at 569 rpm (100%) in helicopter and conversion modes. Once fully converted to airplane mode, the rotor speed is decreased to 478 rpm. The flapping frequency is slightly above 1/rev in a vacuum, although the rotating system frequency is about 0.9/rev, when aerodynamics are included. The fixed system inplane frequency shown in the table is the regressing inplane mode. While the rotor is stiff-inplane to preclude ground resonance, the regressing inplane mode frequency is close to the airframe frequencies and is important for proprotor stability.

9. LINEAR FLIGHT CONTROL SYSTEM MODEL

The BA 609 utilizes a state-of-the-art digital fly-by-wire control system. The pilot has a conventional cyclic stick and pedals, as well as a collective/power lever that controls the vertical axis in helicopter mode and forward speed in airplane mode. The vertical axis control is similar to a conventional helicopter collective in that pulling on the handle increases rotor collective and engine power. The FCS includes rate, attitude, and linear acceleration feedback for handling qualities. Engine torque and rotor rpm feedback are used to maintain rotor speed and power setting. The controls include the two conventional fixed-surface controls (flaperon and elevator) as well as rotor collective, longitudinal cyclic, and engine power setting. The rotor controls can be moved symmetrically or antisymmetrically. Note that the aircraft does not have a rudder or rotor lateral cyclic control. The model includes sensor dynamics, digital delay approximations, and actuator dynamics to achieve good fidelity at the structural mode frequencies.

The FCS has airspeed and nacelle angle scheduling to change the control sensitivity and mixing with flight condition. Ref. 16 describes the development of the BA 609 control architecture and control laws. Structural notch filters are included in the FCS to reduce coupling with structural modes as required.

10. PILOT BIOMECHANICAL RESPONSE

On the V–22, the pilot biomechanical response created three separate divergent oscillations as described in Ref. 11. These oscillations were not anticipated on the V–22 and resulted in delays at flight test as design

solutions were developed and implemented. On the BA 609, the stability methodology has benefited from the V–22 experience and thus included pilot coupling from the start.

The primary difficulty is determining what the pilot biomechanical response will be for a given cockpit and control geometry. On the V–22, the response was measured on the actual aircraft with various pilots. On the BA 609, the pilot response is based on the measured V–22 response with some adjustments for differences in the control geometry.

Typically, pilot response is quantified in terms of inches of stick response per g of acceleration. Fig. 7 shows the V–22 longitudinal pilot model and the measured response data. The open symbols are the measured ground shake test response for two different pilots. As indicated by the response, the pilot biomechanical response can be characterized as a highly damped second order system with a natural frequency between 3 and 4 Hz. There are limited flight test data that support the ground shake test data. A second order transfer function was curve fit to match the measured pilot response, which is referred to as a pilot model. This model is only valid above 1 Hz and should not be confused with the low-frequency pilot models, which predict how the pilot flies the aircraft. On the V–22 and BA 609 there is a lateral control stick balance weight. Because these weights and their moment arms are different on the BA 609 and V–22, an analytical model was tuned to match the measured V–22 data and then modified to represent the BA 609 control properties. For the BA 609 longitudinal cyclic, lateral cyclic, and collective/power lever, pilot biomechanical models were developed and used in the stability analysis. The validity of these models will be verified during the BA 609 testing.

The three pilot models are included as additional feedback paths in the ASAP FCS model. Fig. 8 shows these feedback paths. The pilot models are formulated to represent a high-gain, worse-case pilot. Typically, the actual measured pilot gain will be less than predicted by the models.

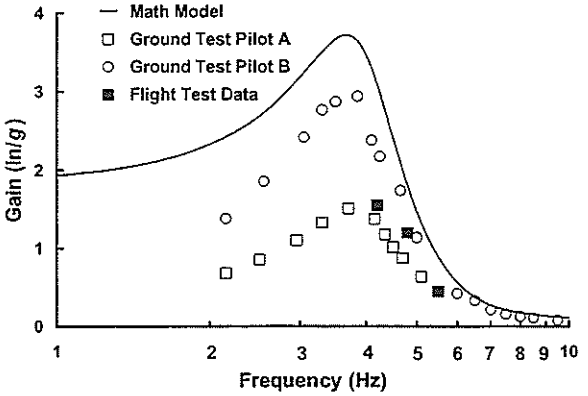

Fig. 7. Measured V–22 longitudinal cyclic stick pilot biomechanical response.

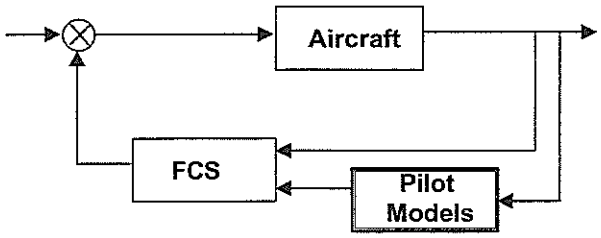

Fig. 8. Pilot feedback block diagram.

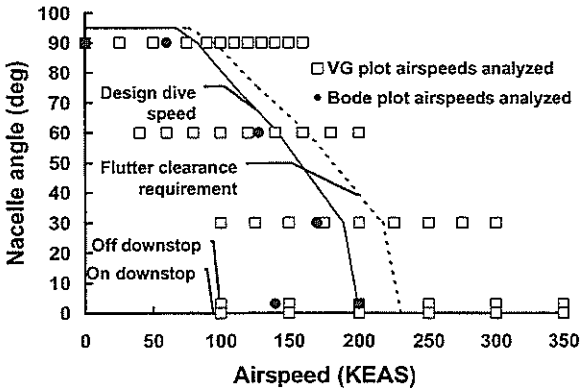

Fig. 9. BA 609 flight envelope at 569 rpm.

11. BA 609 FLIGHT ENVELOPE

The flight envelope for the BA 609 is typically specified separately for helicopter/conversion mode and airplane mode. As forward speed increases from hover, the pilot tilts the nacelles forward. Cockpit displays for the pilot show where the aircraft is within the conversion corridor. Fig. 9 shows the flight envelope for helicopter/conversion modes. Also shown are the stability analysis points. Altitude and gross weight restrictions also limit the conversion corridor of the BA 609. At maximum gross weight during helicopter/conversion mode, the flight envelope has a maximum ceiling of 8,000 ft (2,438 m). The aircraft is capable of flying to 14,000 ft (4,267 m) in conversion mode; however, this capability requires lighter gross weights.

When the nacelles are fully converted, the nacelles are preloaded into a downstop, which provides additional pylon stiffness for high-speed airplane mode flight. Once the downstop is engaged, the rotor speed is reduced from 569 rpm to 478 rpm. The airplane mode flight envelope versus altitude is shown in Fig. 10, which shows the operating ceiling of 25,000 ft (7,700 m). Also included in this figure are the stability analysis data points.

12. STABILITY PREDICTIONS

The analytical stability predictions for the BA 609 were obtained using the methodology described above. The flowchart shown in Fig. 2 summarizes the approach used to ensure that the stability requirements are satisfied. The ASAP computer code is used to calculate eigenvalues for coupled wing, rotor, and drive system as a function of airspeed. Several altitude and gross weight combinations are analyzed to ensure that the basic aircraft has sufficient

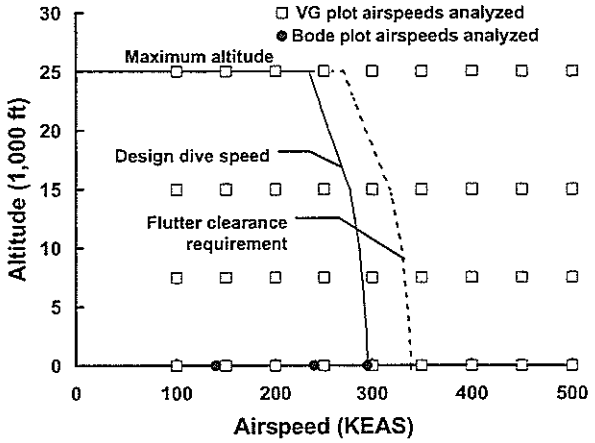

Fig. 10. BA 609 flight envelope at 478 rpm.

stability margins over the entire flight envelope. The basic aircraft frequency and damping versus airspeed for the critical 16,000 lb (7,250 kg) gross weight configuration at sea level standard condition are shown in Fig. 11. To verify that the aircraft is stable for the entire gross weight range, the stability is also verified at the empty gross weight of 11,000 lb (4,990 kg). The symmetric wing chord (SWC) is shown to be critical at 364 knots (674 km/h). The regulations require a 15% margin above the design speed for flutter clearance. Since the predicted point of instability (364 kn [674 km/h]) is greater than the flutter clearance speed (339 kn = 1.15 × 295 kn), the basic aircraft satisfies the stability requirement.

Fig. 11 does not show the frequency and damping for the rotor modes that are included in the analysis. Particularly in high-speed airplane mode, the rotor flap lag stability is important. Fig. 12 shows the rotating system stability for the rotor flapping and inplane modes. Note that the flapping mode is below 1/rev because of the negative spring effect of the negative δ_3. This reduces the flapping frequency to keep it separated from the inplane mode, but does not cause static divergence of the rotor. The damping plot shows that both modes are well damped.

With these requirements satisfied, the linearized flight control system model is then included in the analysis. The FCS bandwidth is high enough for the FCS to interact with the elastic modes of the airframe. Bode plots are generated for each path to verify that the system has acceptable gain and phase margins at the elastic mode frequencies. Although there are no certification requirements for gain and phase margins, 6 dB and 60 degree margins are maintained to ensure a robust design. If the margins are not acceptable, structural filters are added to attenuate the FCS coupling with the structural modes. A typical Bode plot for the aircraft roll rate path is shown in Fig. 13, which shows the gain in the aircraft open loop roll rate path before and after a filter was added. The AWC and AWT modes have gain margins above zero dB without the filter. Therefore, a structural filter is required to reduce FCS coupling to meet the gain margin requirement. The structural notch filter designed for the roll rate path is shown in Fig. 14. This filter reduces the gain at

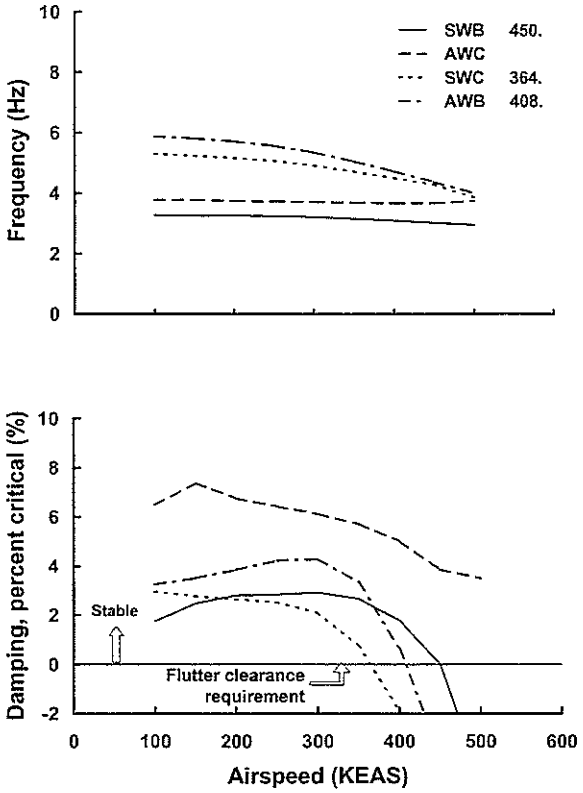

Fig. 11 Airplane mode frequency and damping versus airspeed at sea level standard.

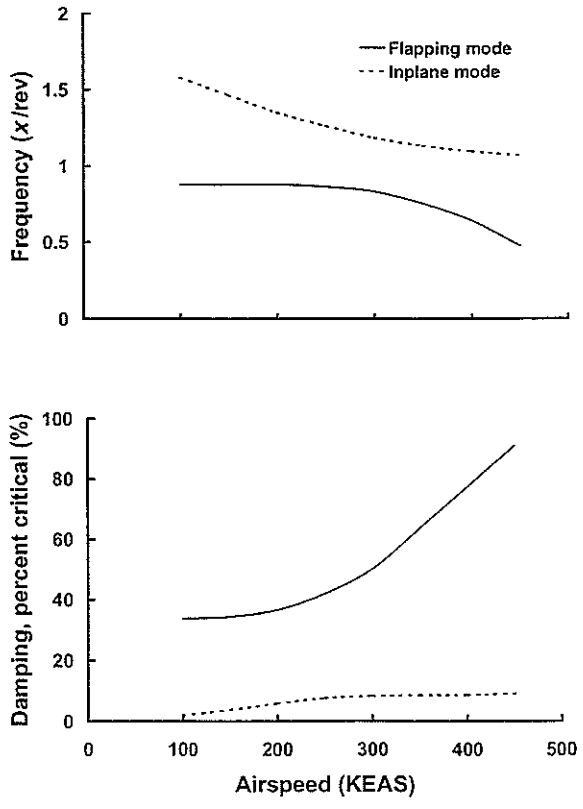

Fig. 12. Rotor flap/lag stability.

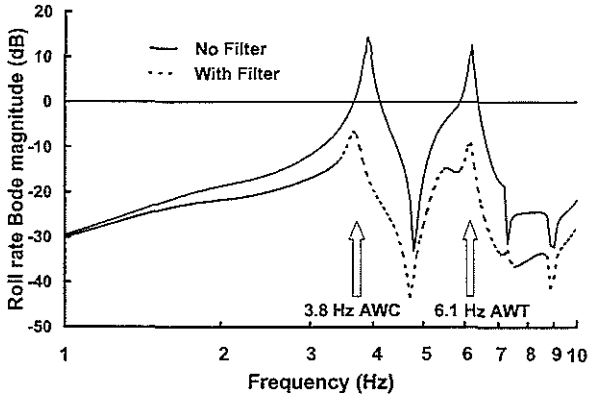

Fig. 13. Airplane mode roll rate Bode plot.

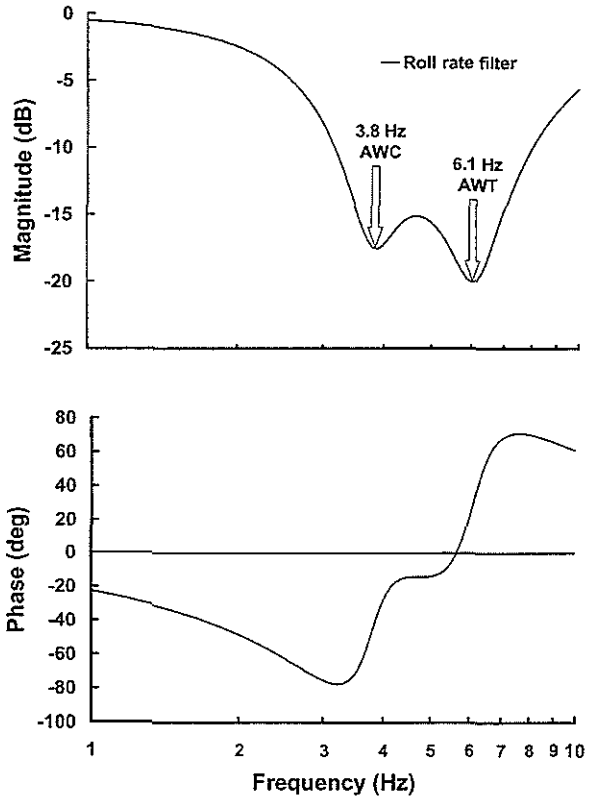

Fig. 14. Airplane mode roll rate filter.

the AWC and AWT mode frequencies by 17.5 and 20 dB, respectively. This filter consists of two second-order notch filters in series. Notch filters are used because they have less phase lag at low frequencies than a second order lag, for example. The phase lag at low frequencies will impact and degrade the handling qualities of the aircraft. Filters placed in the pilot feed forward path can potentially cause phase lags, which may increase the PIO tendency of the aircraft. Similar filters are designed for the other paths, which include

- Longitudinal cyclic stick
- Lateral cyclic stick
- Pitch rate
- Lateral acceleration

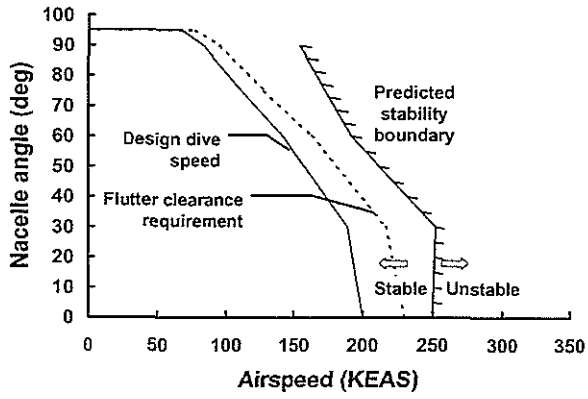

Fig. 15. BA 609 stability boundary and requirements at 569 rpm.

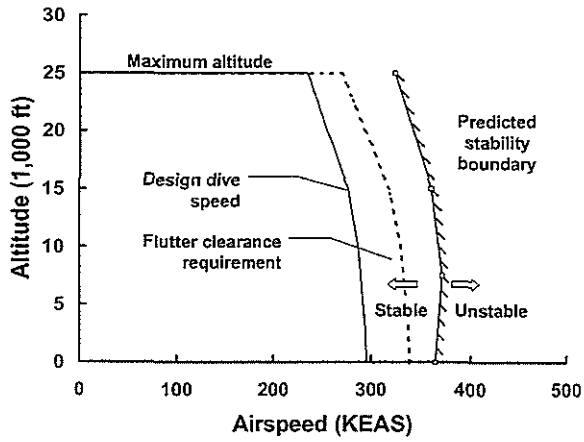

Fig. 16. BA 609 stability boundary and requirements at 478 rpm.

- Power lever
- Yaw rate
- RPM error

Once the filters are defined, the FCS paths are closed and the closed loop aeroelastic stability is evaluated with the effect of the FCS. Fig. 15 shows the helicopter/conversion mode stability predictions at sea level standard conditions and 100% rpm. Sea level standard condition was selected, since previous analysis showed this altitude to be critical. Similarly, closed-loop stability predictions in airplane mode are calculated and compared with the flutter clearance envelope. Fig. 16 shows the airplane mode stability predictions at various altitudes. Based on this analysis, the BA 609 meets all the stability requirements over the complete flight envelope.

In addition to the wing and rotor modes, the FCS can affect the symmetric drive system modes. The first symmetric drive system mode is at 6.70 Hz, which is within the bandwidth of the FCS. ASAP showed that the rpm governor degrades the stability of this mode (Fig. 17). While this mode is predicted to be stable, a filter was added to satisfy the open loop gain margin requirements. Because the filter reduces the coupling of the rpm

governor portion of the FCS, the damping with the filter is more like the basic system.

Classical ground resonance is avoided on the BA 609 by use of a stiff inplane rotor. However, the V-22 experienced a divergent oscillation on the ground caused by pilot biomechanical feedback (Ref. 11). Stability of the XV–15 has not been affected by pilot biomechanical coupling because it used mechanical control linkages instead of fly-by-wire controls. A separate stability analysis was performed on the ground to verify that the BA 609 does not have a ground oscillation like the V-22. On the ground, the airframe dynamics are represented by a rigid aircraft on flexible landing gear and tires. There are two lateral roll modes of the aircraft on its landing gear, and the second mode with a roll pivot point above the aircraft cg is a stability concern. This mode is referred to as the high-focus roll mode. The ASAP analysis has been correlated extensively with V–22 onground data to accurately predict the damping in this mode. Because this mode of the rigid aircraft on the gear and tires (1.82 Hz) is very low, it is difficult to stabilize this mode with only a notch filter without significantly degrading the aircraft handling qualities. Therefore, a lateral balance weight is used in the mechanical controls to reduce the sensitivity of the pilot lateral stick input to cockpit lateral acceleration. This allows a smaller filter to be used in the lateral stick feed forward path without degrading the handling qualities.

Fig. 18 shows the basic aircraft predicted damping for the onground, high-focus roll mode. The basic aircraft is stable as shown. With the FCS and pilot biomechanical feedback, the aircraft is unstable. The combination of a filter and balance weight stabilizes this onground mode.

13. SUMMARY AND CONCLUSIONS

Bell has developed a comprehensive methodology to evaluate aeroelastic and aeroservoelastic stability, which has been applied successfully to the V–22 and XV–15. This analysis shows that the BA 609 will satisfy all of the aeroelastic and aeroservoelastic stability requirements. Specifically for the BA 609, the following conclusions can be made:

1. Acceptable airplane mode proprotor stability speeds are met primarily because of the high torsional stiffness in the wing.
2. Ground resonance can be avoided by using a stiff-inplane rotor.
3. High-speed flap lag instability can be avoided by using negative δ_3.
4. Coupling of the flight control system with the structural modes can be reduced using notch filters without introducing unacceptable low-frequency phase delays.
5. The adverse effect of pilot biomechanical coupling on stability can be reduced by using notch filters in the FCS and a balance weight in the mechanical controls.
6. Torsional stability is maintained by appropriate filtering of the rotor rpm error feedback.

14. REFERENCES

1. K. G. Wernicke, "Tilt Proprotor Composite Aircraft, Design State of the Art," 24th Annual Forum of the American Helicopter Society, May 1968.
2. T. M. Gaffey, J. G. Yen, and R. G. Kvaternik, "Analysis and Model Tests of the Proprotor Dynamics of a Tilt-Rotor VTOL Aircraft," V/STOL Technology and Planning Conference, Las Vegas, Nevada, September 1969.
3. Raymond G. Kvaternik, "Experimental and Analytical Studies in Tilt-Rotor Aeroelasticity," AHS/NASA Ames Specialist Meeting on Rotorcraft Dynamics, February 1974.
4. Kipling Edenborough, Troy M. Gaffey, and James A. Weiberg, "Analysis and Tests Confirm Design of Proprotor Aircraft," AIAA 4th Aircraft Design, Flight Test, and Operations Meeting, Los Angeles, CA, August 1972.
5. Mark W. Nixon, "Parametric Studies for Tiltrotor Aeroelastic Stability in Highspeed Flight," 33rd Structures, Structural Dynamics, and Materials Conference, April 1992, Dallas, TX.

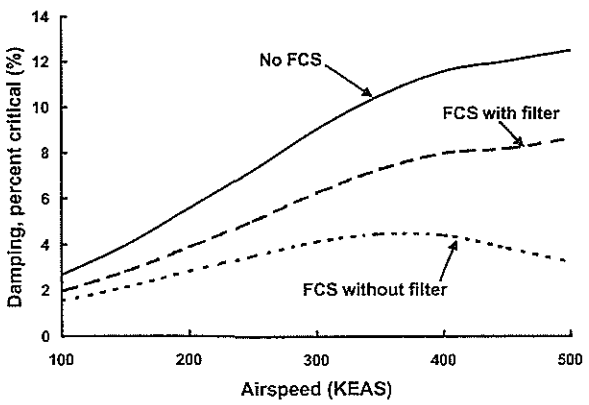

Fig. 17. First symmetric drive system mode stability.

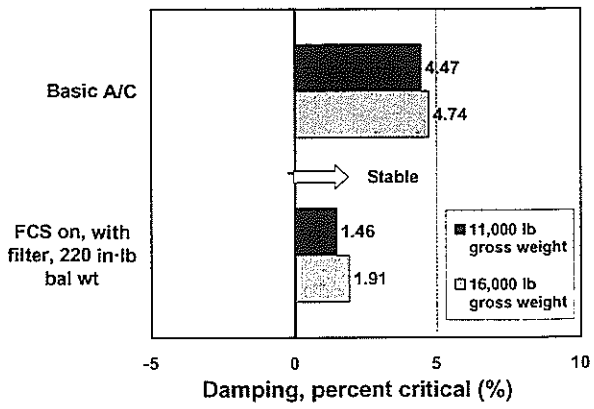

Fig. 18. Onground high-focus roll mode stability.

6. Michael J. Moore, et. al., "High Speed Tiltorotors: Dynamics Methodology," 49th Annual Forum of the American Helicopter Society, St. Louis Missouri, May 1993.
7. Lawrence M. Corso, et. al., "Design, Analysis, and Test of a Composite Tailored Tiltrotor Wing," 53rd Annual Forum of the American Helicopter Society, Virginia Beach, Virginia, April–May 1997.
8. J. M. Bilger, R. L. Marr, and Ahmad Zahedi, "Results of Structural Dynamic Testing of the SV–15 Tilt Rotor Research Aircraft," 37th Annual Forum of the American Helicopter Society, New Orleans, LA, May 1981.
9. Roman T. Lytwyn, "An Analysis of the Divergent Vertical Helicopter Oscillations Resulting from the Physical Presence of the Pilot in the Collective Control Loop," *Journal of the American Helicopter Society*, Vol. 12 (1), Jan 1967.
10. Thaddeus Kaplita, et. al., "Helicopter Simulation Development by Correlation with Frequency Sweep Flight Test Data," 45th Annual Forum of the American Helicopter Society, Boston, MA, May 1989.
11. Tom Parham, et. al., "V–22 Pilot-In-The-Loop Aeroelastic Stability Analysis," 47th Annual Forum of the American Helicopter Society, Phoeniz, AZ, May 1991.
12. Robert F. Idol and Tom Parham, "V–22 Aeroelastic Stability Analysis and Correlation with Test Data," 51st Annual Forum of the American Helicopter Society, Fort Worth, Texas, May 1995.
13. David Popelka, et. al., "Correlation of Stability test Results and Analysis for the 1/5 Scale V–22 Aeroelastic Model," 41st Annual Forum of the American Helicopter Society, Fort Worth, Texas, May 1985.
14. Wayne Johnson, *Helicopter Theory*, Princeton University Press, 1980.
15. Troy M. Gaffey, "The Effect of Positive Pitch-Flap Coupling (Negative δ_3 on Rotor Blade Motion Stability and Flapping)," 24th Annual Forum of the American Helicopter Society, May 1968.
16. R. L. Fortenbaugh, D. King, M. A. Peryea, and T. Busi, "Flight Control Features of the Bell Agusta (BA) 609: A Handling Qualities Perspective," 25th European Rotorcraft Forum, September 1999.